This is a preprint, the final version is subject to change, of the American Mineralogist (MSA)
Cite as Authors (Year) Title. American Mineralogist, in press.
DOI: https://doi.org/10.2138/am-2018-6447

Revision2

Why natural monazite never becomes amorphous: experimental evidence for alpha self-healing.

Anne-Magali Seydoux-Guillaume[1,2], Xavier Deschanels[3], Cédric Baumier[4], Stefan Neumeier[5], William John Weber[6,7], and Sylvain Peuget[8].*

[1] CNRS, Université Clermont Auvergne, IRD, UJM, Laboratoire Magmas et Volcans, F-63000 Clermont-Ferrand, France

[2] Univ Lyon, UJM-Saint-Etienne, UCA, CNRS, IRD, LMV UMR 6524, F-42023 SAINT-ETIENNE, France

[3] ICSM, CEA, CNRS, ENSCM, Univ Montpellier, Marcoule, France

[4] CSNSM, JANNuS-Orsay/SCALP, Univ Paris-Sud, CNRS/IN2P3, Orsay, France

[5] Forschungszentrum Jülich GmbH, Institute of Energy and Climate Research, Nuclear Waste Management and Reactor Safety (IEK-6), D-52425 Jülich, Germany

[6]Department of Materials Science and Engineering, University of Tennessee, Knoxville, TN 37996, USA

[7] Materials Science and Technology Division, Oak Ridge National Laboratory, Oak Ridge, TN 37831, USA

[8] CEA, DEN, DE2D, SEVT, LMPA BP 17171, 30207 Bagnols-sur-Ceze Cedex, France.

*Corresponding author.

*E-mail address:*anne.magali.seydoux@univ-st-etienne.fr (A.-M. Seydoux-Guillaume).

ABSTRACT:

Monazite, a common accessory rare-earth orthophosphate mineral in the continental crust widely used in U-Pb geochronology, holds promise for (U-Th)/He thermochronology, and for the immobilization of Pu and minor actinides (MA) coming from spent nuclear fuel

reprocessing. Previous results obtained on natural and plutonium-doped monazite have demonstrated the ability of this structure to maintain a crystalline state despite high radiation damage levels. However, the low critical temperature (180°C), above which amorphization cannot be achieved in natural monazite under ion irradiation, does not explain this old and unsolved paradox: why do natural monazites, independent of their geological history, remain crystalline even when they did not experience any thermal event that could heal the defects? This is what the present study aims to address. Synthetic polycrystals of $LaPO_4$-monazite were irradiated sequentially and simultaneously with alpha particles (He) and gold (Au) ions. The use of Au^{2+} ions at 1.5 MeV allows the simulation of the nuclear energy loss of the recoil nucleus and He^{+} ions at 160 keV simulate the electronic energy loss of the α-particle released in α-decay. *In situ* irradiation experiments were performed at room temperature conditions on the JANNuS-Orsay/SCALP platform, which couples two accelerators with a Transmission Electron Microscope. Our results demonstrate experimentally for the first time in monazite, the existence of the defect recovery mechanism, called alpha-healing, acting in this structure due to electronic energy loss of alpha particles, which explains the absence of amorphization in natural monazite samples. This mechanism is critically important for monazite geo and thermochronology and to design and predictively model the long-term behavior of ceramic matrices for nuclear waste conditioning.

Keywords: monazite; alpha self-healing; *in situ* TEM irradiation; dual-ion beam irradiation; Helium; geo and thermochronology; nuclear waste

INTRODUCTION

Monazite (APO_4, A = LREE, Th, U, Ca; Clavier et al., 2011), is a common accessory rare-earth orthophosphate mineral in the continental crust widely used in U-Pb geochronology

(Parrish, 1990). It is also a promising candidate for the immobilization of Pu (for countries that are not actively reusing Pu in MOX fuel) and minor actinides (MA) coming from spent nuclear fuel reprocessing (Boatner et al., 1988; Weber et al., 1998), due to its high structural flexibility that can accommodate high concentrations of actinides in its structure, its high chemical durability, and its apparent high-radiation resistance (e.g. Ewing and Wang, 2002; Seydoux-Guillaume et al., 2004; Lumpkin, 2006; Oelkers and Montel, 2008; Dacheux et al., 2013). However, this last point, demonstrated in natural crystals (Seydoux-Guillaume et al., 2004), is still not understood. During an α-decay event, an α-particle (4-8 MeV) and a recoil nucleus (70-165 keV) are released. The kinetic energy of these two particles is deposited in the host material by two distinct processes, ballistic (S_{nucl}) and electronic (S_{elec}). The ballistic process correspond to elastic collisions between atom nuclei, and the electronic process to ionization and electronic processes resulting in a temperature rise in the material. Most of the atomic displacements that can result in amorphization of the crystal lattice are caused by the recoil nuclei (e.g. 1000-2000 atomic displacements) due to intense elastic collision cascades (Ewing et al., 2000). In contrast to its U-Pb geochronological concurrent zircon, which commonly contains U in the hundreds of parts per million range, has received alpha-decay doses on the order of 10^{18}–10^{19} α/g, and is easily amorphized (Ewing et al., 2000), even very old (up to 2 Ga) monazite crystals, containing high concentrations of actinides (up to 10 wt. % ThO_2 and ~1 wt. % UO_2), and thus sustaining high irradiation doses (up to 1.7 x 10^{20} α/g, which should induce up to 14 displacements per atom – dpa), are not amorphous; evidence of radiation damage is limited to isolated nm-sized domains within the crystal, corresponding to strain in the lattice (Seydoux-Guillaume et al., 2004). Similarly, Pu-doped monazite remains crystalline even after an irradiation dose of 7.5x10^{18} α/g (0.8 dpa; Deschanels et al., 2014), which is well above the critical amorphization doses (~0.3 dpa) determined using external heavy-ion irradiation experiments (Meldrum et al., 1996). The reason for this apparent

resistance has remained an enigma until today. It is well known that the critical amorphization temperature, for natural monazite under ion irradiation is relatively low (180°C; Meldrum et al., 1997a) compared to other minerals (e.g. 830°C for zircon, 1130°C for quartz, 440°C for zirconolite; Ewing et al., 2000), and the temperature and activation energy associated with thermal recrystallization of the amorphous state is much lower for monazite (~300°C, 2.7 eV; Karioris et al., 1981; Ehlert et al., 1983; Deschanels et al., 2014) than for zircon (1200°C, 5.3 to 6.6 eV; Weber, 1990). Furthermore, the large differences in dose rates between ion irradiation and Pu-doped or natural monazite are insufficient to explain the amorphization resistance (Deschanels et al., 2014). In monazite, the transition between amorphous and crystalline states is also very sensitive to electron beams and to the ratio of electronic-to-nuclear energy loss (S_{elec}/S_{nucl}) of the accelerated ions (Meldrum et al., 1997b; Deschanels et al., 2014). More generally, other phosphates (F-apatite, berlinite, xenotime) exhibit similar behavior, which is generally attributed to the presence of tetrahedrally coordinated phosphorous and to the higher binding energy of the P-O bond compared to Si-O (Meldrum et al., 1999; Luo and Liu, 2001). However, these results cannot explain the behavioral differences (amorphization, swelling) observed for equivalently damaged monazite resulting from external heavy ion irradiation compared to α-decay self-irradiation (natural monazite or ^{238}Pu doped monazite; Fig. 1 in Supp. Data). Finally, the mechanism called α-healing, experimentally demonstrated for apatite (Ouchani et al., 1998; Soulet et al., 2001; Gerin et al., 2017; Li et al., 2017) and borosilicate glasses (Mir et al., 2015), but only suggested for monazite (Soulet et al., 2001; Seydoux-Guillaume et al., 2002; Deschanels et al., 2014), could be another possibility and remains to be demonstrated. The present experimental study solves the old paradox of the apparent resistance of monazite samples to amorphization, and demonstrates for the first time in monazite the existence and efficiency of α-particles for recovering radiation damage in this mineral.

This is a preprint, the final version is subject to change, of the American Mineralogist (MSA)
Cite as Authors (Year) Title. American Mineralogist, in press.
DOI: https://doi.org/10.2138/am-2018-6447

SAMPLE AND METHODS (MORE DETAILS IN SUPPLEMENTARY DATA)

Several Focused Ion Beam (FIB)-foils (12 x 6 x 0.1 μm) were cut perpendicular to the surface of the polycrystalline sample of sintered monazite ($LaPO_4$) ceramic, by the *in situ* lift-out technique for the Transmission Electron Microscope (TEM) *in situ* irradiation experiments performed at room temperature conditions on the JANNuS-Orsay/SCALP platform, which allows coupling two accelerators with a Transmission Electron Microscope (Figure 5 in Suppl data). We used Au^{2+} ions at 1.5 MeV to simulate the nuclear energy loss of the recoil nucleus of an α-decay ($S_{nucl.}$ ~ 4.5 keV/nm) and He^{+} ions at 160 keV to simulate the electronic energy loss of the α-particle released in α-decay ($S_{elec.}$ ~ 0.254 keV/nm). To evaluate the recovery effect of α-particles on the damage state induced by heavy recoil nuclei, three irradiation configurations were investigated: two were sequential, and the third simultaneous (Figs. 2-3). All three used the same ions and accelerating energy: 1.5 MeV Au^{2+} ions (ARAMIS accelerator) to induce ballistic damage and 160 keV He^{+} ions (IRMA accelerator) to induce electronic excitations without implanting He atoms in the lamella. (For further details see in Supplementary Materials)

RESULTS AND DISCUSSION

In the first experiment (Fig. 2), Au irradiation up to $2x10^{14}$ Au/cm² (1.13 dpa) is used to fully amorphize the monazite sample (Picot et al., 2008; Deschanels et al., 2014), and ten He irradiation steps are subsequently performed up to a fluence of $5x10^{16}$ He/cm² to evaluate the recovery of the fully amorphized material due to electronic energy loss of He ions (Table 1 in Supplementary Material). The second experiment (Fig. 3) is similar to the first and aims at evaluating the He-induced recovery of a partially damaged material (0.2 dpa), corresponding to a monazite with a strained lattice (Deschanels et al., 2014), and structurally similar to natural monazite samples (Seydoux-Guillaume et al., 2004). The third experiment

(Fig. 4) involve simultaneous irradiation by Au and He ions, up to fluences of $2x10^{14}$ Au/cm² and $3.4x10^{16}$ He/cm², performed in 4 steps. All these experiments were performed without continuous TEM observation to avoid artefacts (e.g. recrystallization; see Figs. 6-7 in Suppl. Mat.) from the electron beam (Meldrum et al., 1997b; Deschanels et al., 2014). Therefore, Bright-Field images (BF) and Selective Area Electron Diffraction (SAED) were done rapidly after each irradiation step under conditions carefully chosen (Suppl. Mat.) to avoid any recrystallization of amorphous areas (0.17 nA at x25500 magnification).

The first experiment (#2; Fig. 2) confirms that monazite is completely amorphous at a fluence of $2x10^{14}$ Au/cm² (1.13 dpa), consistent with previous work (Deschanels et al., 2014). At 10^{14} Au/cm² (0.56 dpa), the foil is almost completely amorphous, only a few phantoms of grain boundaries remain (compare Fig. 2A-B). This result is confirmed both by the diffuse rings in the SAED pattern and the homogeneous contrast in the BF image (Fig. 2C). After amorphization, successive steps of He-irradiation were performed. A first modification in the crystallinity of the amorphized monazite appears at $4x10^{16}$ He/cm², where nanometer size nuclei formed in the sample (Suppl. Mat. Fig. 7). Significant changes are observed at $5x10^{16}$ He/cm² with the presence of a greater amount of crystallized nuclei (arrows in Fig. 2D), corresponding to spots in the diffraction pattern (circle in SAED Fig. 2D). This nucleation process is similar to that due to an electron beam (Meldrum et al., 1997b; Deschanels et al., 2014), suggesting an effect of the electronic energy loss from α-particles, since the electron beam contribution in our experiment is negligible (Suppl. Mat. Fig. 7). This observation is confirmed by the achievement of another Au+He sequential irradiation experiment (#5; Fig. 8 in Suppl. Mat.) with 1.5 MeV He (factor of 4 lower $S_{nucl.}$ with similar $S_{elec.}$ than for #2), during which the same recrystallization was observed at similar fluence levels (Suppl. Mat. Fig. 8), ruling out a recovery mechanism involving nuclear energy loss. In contrast, He-irradiation of the partially damaged sample (#3; Fig. 3) induces immediate recovery of the crystallinity at

low He-fluence (from 10^{14} He/cm²; Fig. 3C) with a very efficient recrystallization process (Fig. 3D-E), as attested by the disappearance of amorphous rings and appearance of Bragg diffraction lines, with well-defined bend contours at the end of the He-irradiation cycle ($5x10^{15}$ He/cm²; Fig. 3E). These results are a first demonstration that the electronic energy deposited in the sample during helium irradiation is responsible for the recrystallization of monazite, either inducing nucleation and growth (Fig. 2D) when starting with an amorphized material, or inducing a recovery of the defected structure when starting with a partially damaged monazite (Fig. 3B-E).

Results from the dual-ion beam experiment (Fig. 4) distinctly demonstrate that simultaneous irradiation with He and Au prevents monazite from undergoing amorphization, as the sample remains crystalline at Au fluences that induced full amorphization in experiment 1 (Figs. 4C-D). The only visible changes are modifications in the bright field contrasts, corresponding to small lattice distortion and presence of strains (i.e. Bragg lines are different in Figs. 4B-C-D); however, the global orientation is approximately the same in both SAED patterns when the doses increase from 10^{14} to $2x10^{14}$ Au/cm² (Figs. 4C-D). Another modification corresponds to the formation of mottled diffraction contrasts (Fig. 4D), typical of point defect formation due to ballistic process, which are commonly observed in natural monazite samples (e.g. Seydoux-Guillaume et al., 2003, 2004, 2018) or in monazite samples irradiated at lower Au-fluences (~ 0.05 dpa in Deschanels et al., 2014). The last proof that helium irradiation prevents monazite amorphization is shown in Figs. 4E-F. The bottom right area of the foil (Fig. 4E) corresponds to a region where the helium beam was masked (only irradiated by Au ions) and that is completely amorphous, as shown by the homogeneous BF-contrast and the diffuse rings in SAED pattern (Fig. 4E-F).

IMPLICATIONS

From our results, it can be concluded that during α-decay self-irradiation of monazite a competition takes place between (1) damage creation by ballistic processes induced by recoil nuclei, resulting in atomic displacements and defect formation, and (2) electronic processes from α-particle ejection, from which the electronic energy deposited in the material is sufficient to heal the displaced atoms and prevents the structure amorphization. This mechanism, called α-healing, finally explains why monazite is never amorphous in nature, independent from its thermal history: the α-particles are able to heal the damage generated by the recoil nuclei, via a thermal spike induced by the electronic energy loss (Weber et al., 2015; Zhang et al., 2015) and prevent amorphization.

Our results have different implications, especially in geochronology (U-Pb and Th-Pb), thermochronology (fission tracks and U-Th/He), and for the containment of actinides in monazite matrix. First, this mechanism explains what is long known about monazite U-Pb and Th-Pb dating, i.e. disturbance of the geochronological systems is not due to Pb diffusion (Seydoux-Guillaume et al., 2002). Pb diffusion coefficient obtained from experimental studies performed in synthetic monazite crystals (Cherniak et al., 2004; Gardès et al., 2006) must be very close to the Pb diffusion coefficient that would be measured from natural monazite samples. With the help of alpha-healing mechanisms, monazite can be continuously maintained in a crystalline state during its geological history even at low temperature. Our results confirms then, that, in contrast to zircon where amorphization is very common and in which Pb loss by diffusion can be enhanced, significant Pb loss in monazite will not happen via diffusion; the U-Pb and Th-Pb systems will remain closed at the μm scale, and thus grain size scale, and disturbance of U-Pb and Th-Pb systems can only happens via dissolution-precipitation mechanisms (Seydoux-Guillaume et al., 2018). However, at the nanoscale, Pb mobility could be locally and temporary enhanced due to defect formation before defect healing, and may be responsible for Pb segregation into nanophases observed at the nanoscale

in monazite (e.g. Seydoux-Guillaume et al., 2003; Fougerouse et al., 2018); this should be studied in details, taking into account this new alpha-healing mechanism active in monazite.

Secondly, the knowledge of He diffusivity is crucial in (U-Th/He) thermochronology for the estimation of closure temperature (T_c), to give correct interpretation of thermal history (e.g. Farley and Stockli, 2002; Cherniak and Watson, 2013). In apatite, it has been demonstrated that vacancies can efficiently trap He atoms, thus reducing diffusivity (Gerin et al., 2017). In monazite, the differences in He diffusivities, and therefore in T_c (~100°C difference according to authors; Peterman et al., 2014), depending on the type of samples (natural vs synthetic) and the type of experiments (step heating vs ^{3}He implantation) may be a consequence of the amount of radiation damage in monazite, which depends on the healing effect of He, as demonstrated in our study. Furthermore, ^{3}He implantation (100 keV, 5 x 10^{15} He/cm²) used for He diffusivity measurements in natural monazite (Cherniak and Watson, 2013) may induce some recovery of radiation damage as these conditions are very similar to those used in our present study (160 keV, recovery from 10^{14} He/cm²; Fig. 3) and may explain discrepancies between authors using step heating (see Fig. 3 in Peterman et al., 2014), and a much less pronounced difference in He-diffusivities between natural and synthetic monazite for Cherniak and Watson (2013) than for Farley (2007). Our results have therefore demonstrated the necessity to consider α-healing in experimental set-up and models used for U-Th/He thermochronology. Length measurements of confined fission tracks in monazite should also be taken with care because the efficiency of the α-healing is not considered in the thermal annealing models. Even at ambient temperature, healing of tracks may reduce the track length and make interpretation of thermochronological data difficult (Weise et al., 2009). Furthermore, to correlate the amount of radiation damage in natural monazite samples to the temperature at which they were exposed, should be avoided, as α-healing proceeds

independently from thermal history; low-temperature damage annealing has to be excluded as an explanation of radiation resistance of natural monazite samples.

Finally, our results have important implications for the Pu and MA immobilization in monazite matrices because it implies that the α-particles produced by α-decays are sufficient to heal the structure damaged by self-irradiation due to recoil nuclei. Such a mechanism acting in the monazite structure should prevent the matrix from amorphization and microcracking as a consequence of swelling. The benefit is evident for the long-term behavior of monazite as a nuclear waste matrices, because the leaching rate would not be altered by radiation damage since the atomic structure and the specific surface area of the material would be conserved.

ACKNOWLEDGMENTS:

Experiment performed at the CSNSM facility: JANNuS-Orsay/SCALP platform (CSNSM Univ Paris-Sud / CNRS, Orsay, France). We thank V. Picot-Magnin (ISTerre, CNRS, France) for the synthesis of monazite samples. This experiment was supported by the EMIR French accelerator network. This work was partly supported by the french RENATECH network. Two of the authors were supported by the U.S. Department of Energy, Office of Basic Energy Sciences, Materials Science and Engineering Division (WJW) and the German Federal Ministry of Education and Research (BMBF), grant no. 02NUK021A (SN), respectively. NEEDS-CNRS is thanked for financial support. E. Gardès is thanked for the long and exciting discussion on diffusion. Two anonymous reviewers are thanked for their constructive comments. The associated editor, Ian Swainson, is also thanked for his helpful editorial handling.

REFERENCES:

Boatner, L.A., and Sales B.C. (1988) Monazite. In Radioactive Waste Forms for the Future. Lutze W, Ewing RC, Eds. North-Holland, Amsterdam, 495–564.

Cherniak, D.J., and Watson, E.B. (2013) Diffusion of helium in natural monazite, and preliminary results on He diffusion in synthetic light rare earth phosphates. American Mineralogist, 98, 1407-1420.

Clavier, N., Podor, R., and Dacheux, N. (2011) Crystal chemistry of the monazite structure. Journal of European Ceramic Society, 31, 941-976.

Dacheux, N., Clavier, N., and Podor, R. (2013) Monazite as a promising long-term radioactive waste matrix: benefits of high-structural flexibility and chemical durability. American Mineralogist, 98, 833-847.

Deschanels, X., Seydoux-Guillaume, A.M., Magnin, V., Mesbah, A., Tribet, M., Moloney, M., Serruys, Y., and Peuget, S. (2014) Swelling induced by alpha decay in monazite and zirconolite ceramics: a XRD and TEM comparative study. Journal of Nuclear Materials, 448, 184-194.

Ehlert, T.C., Appaji Gowda, K., Karioris, F.G., and Cartz, L. (1983) Differential scanning calorimetry of heavy ion bombarded synthetic monazite. Radiation Effects, 70, 173-181.

Ewing, R.C., and Wang, L.M. (2002) Phosphates as nuclear waste forms. In Kohn, M.J., Rakovan, J., and Hughes, J.M. Eds, Phosphates: Geochemical, Geobiological, and Materials importance, 48, pp. 673–699. Reviews in mineralogy and geochemistry, Mineralogical Society of America, Washington DC.

Ewing, R.C., Meldrum, A., Wang, L.M., and Wang, S.X. (2000) Radiation induced amorphization. In Redfern, S.A.T., and Carpenter, M.A., Eds, Transformation processes in

minerals, 39, pp. 319-361. Reviews in Mineralogy and Geochemistry, Mineralogical Society of America, Washington DC.

Ewing, R.C., Weber, W.J., and Clinard, F.W. Jr. (1995) Radiation effects in nuclear waste forms. Progress in Nuclear Energy, 29, 63-127.

Farley, K.A. (2007) He diffusion systematics in minerals: Evidence from synthetic monazite and zircon structure phosphates. Geochimica et Cosmochimica Acta, 71, 4015-4024.

Farley, K.A., and Stockli, D.F. (2002) (U-Th)/He dating of phosphates: apatite, monazite, and xenotime. In D. Porcelli, C.J. Ballentine, and R. Wieler, Eds., Noble Gases in Geochemistry and Cosmochemistry, 47, p. 559–577. Reviews in Mineralogy and Geochemistry, Mineralogical Society of America, Washington DC.

Fougerouse D., Reddy S.M., Saxey D.W., Erickson T.M., Kirkland C.L., Rickard W.A., Seydoux-Guillaume A.M., Clark C., Buick I.S. (2018). Nanoscale distribution of Pb in monazite revealed by atom probe microscopy. Chemical Geology doi:10.1016/j.chemgeo.2018.01.020.

Gerin, C., Gautheron, C., Oliviero, E., Bachelet, C., Mbongo-Djimbi, D., Seydoux-Guillaume, A.M., Tassan-Got, L., Sarda, P., Roques, J., Garrido, F. (2017) Influence of vacancy damage on He diffusion in apatite, investigated at atomic to mineralogical scales. Geochimica et Cosmochimica Acta, 197, 87-103.

Karioris, F.G., Appaji Gowda, K., and Cartz, L. (1981) Heavy ion bombardment of monoclinic ThSiO4, ThO2 and monazite. Radiation Effects Letters, 58, 1-3.

Li, W., Shen, Y., Zhou, Y., Nan, S., Chen, C.-H., and Ewing, R.C. (2017) In situ TEM observation of alpha particle induced annealing of radiation damage in Durango apatite. Scientific Report, 7, 14108.

Luo, J.S., and Liu, G.K. (2001) Microscopic effects of self-radiation damage in ^{244}Cm-doped $LuPO_4$ crystals. Journal of Material Research, 16, 366-372.

Lumpkin, G.R. (2006) Ceramic waste forms for actinides. Elements, 2, 365-372.

Meldrum, A., Boatner, L.A., and Ewing, R.C. (1997a) Displacive radiation effects in the monazite-and zircon-structure orthophosphates. Physical Review B, 13805-13814.

Meldrum, A., Boatner, L.A., and Ewing, R.C. (1997b) Electron-irradiation- induced nucleation and growth in amorphous $LaPO_4$, $ScPO_4$, and zircon. Journal of Material Research, 12, 1816-1827.

Meldrum, A., Wang, L.M., and Ewing, R.C. (1996) Ion-beam-induced amorphization of monazite. Nuclear Instruments and Methods B, 116, 220-224.

Meldrum, A., Zinkle, S.J., Boatner, L.A., and Ewing, R.C. (1999) Heavy-ion irradiation effects in the ABO_4 orthosilicates: decomposition, amorphization, and recrystallization. Physical Review B, 59, 3981-3992.

Mir, A.H., Peuget, S., Toulemonde, M., Bulot, P., Jegou, C., Miro, S., and Bouffard, S. (2015) Defect recovery and damage reduction in borosilicate glasses under double ion beam irradiation. EPL, 112, 36002.

Oelkers, E.H., and Montel, J.-M. (2008) Phosphates and nuclear waste storage. Elements, 4, 113-116.

Ouchani, S., Dran, J.-C., and Chaumont, J. (1998) Exfoliation and diffusion following helium ion implantation in fluorapatite: implications for radiochronology and radioactive waste disposal. Applied Geochemistry, 13, 707-714.

Parrish, R.R. (1990) U-Pb dating of monazite and its application to geological problems. Canadian Journal of Earth Science, 27, 1431-1450.

Peterman, E.M., Hourigan, J.K., and Grove, M. (2014) Experimental and geologic evaluation of monazite (U–Th)/He thermochronometry: Catnip Sill, Catalina Core Complex, Tucson, AZ. Earth and Planetary Science Letters, 403, 48-55.

Picot, V., Deschanels, X., Peuget, S., Glorieux, B., Seydoux-Guillaume, A.M., and Wirth R. (2008) Ion beam radiation effects in monazite. Journal of Nuclear Materials, 381, 290-296.

Reiners, P.W., Carlson, R.W., Renne, P.R., Cooper, K.M., Granger, D.E., McLean, N.M., and Schoene, B. (2018) Geochronology and Thermochronology, 480 pp., Wiley, ISBN: 978-1-118-45585-2.

Seydoux-Guillaume, A.M., Goncalves, P., Wirth, R., and Deutsch, A. (2003) TEM study of polyphasic and discordant monazites: site specific specimen preparation using the Focused Ion Beam technique. Geology, 31, 973-976.

Seydoux-Guillaume, A.M., Wirth, R., Deutsch, A., and Schärer, U. (2004) On the microstructure of up to 2 Ga old concordant monazites: a X-ray diffraction and transmission electron microscope study. Geochimica et Cosmochimica Acta, 68, 2517-2527.

Seydoux-Guillaume, A.M., Wirth, R., Nasdala, L., Gottschalk, M., Montel, J.M., and Heinrich, W. (2002) An XRD, TEM and Raman study of experimentally annealed natural monazite. Physics and Chemistry of Minerals, 29, 240-253.

Seydoux-Guillaume, A-M, Bingen, B., Bosse, V., Janots, E., and Laurent, A.T. (2018). Transmission Electron Microscope imaging sharpens geochronological interpretation of zircon and monazite. vol. Geophysical Monograph 232, p.261-275, Microstructural Geochronology: Planetary Records Down to-Atom Scale.

Soulet, S., Carpena, J., Chaumont, J., Kaitasov, O., Ruault, M.-O., and Krupa, J.C. (2001). Simulation of the alpha-annealing effect in apatitic structures by He-ion irradiation: influence of the silicate/phosphate ratio and of the OH/F substitution. Nuclear Instruments and Methods, B, 184, 383–390.

Weber, W.J., Ewing, R.C., Catlow, C.R.A., de la Rubia, T.D., Hobbs, L.W., Kinoshita, C., Matzke, H., Motta, A.T., Nastasi, M., Salje, E.K.H., Vance, E.R., and Zinkle, S.J. (1998) Radiation effects in crystalline ceramics for the immobilization of high-level nuclear waste and plutonium. Journal of Material Research, 13, 1434-1484.

Weber, W.J. (1990) Radiation-induced defects and amorphization in zircon. Journal of Material Research, 5, 2687-2697.

Weber, W.J., Duffy, D.M., Thomé, L., and Zhang, Y. (2015) The role of electronic energy loss in ion beam modification of materials. Curr. Opin. Solid State Mater. Sci. 19, 1-11.

Weise, C., van den Boogaart, K., Jonckheere, R., and Ratschbacher, L. (2009) Annealing kinetics of Kr-tracks in monazite: Implications for fission-track modelling. Chemical Geology, 260, 129-137.

Zhang, Y., Sachan, R., Pakarinen, O.H., Chisholm, M.F., Liu, P., Xue, H., and Weber, W.J. (2015) Ionization-induced annealing of pre-existing defects in silicon carbide. Nature Communications 6, 8049.

FIGURES CAPTIONS

Figure 2. Bright-Field Transmission Electron Microscope images (BF-TEM) of a sequence of *in situ* irradiation in $LaPO_4$ monazite polycrystal - first experiment: complete amorphization ($2x10^{14}$ Au/cm²). A- Part of the TEM focused ion beam (FIB) foil before irradiation. **B**- Same area as in A *in situ* irradiated up to $1x10^{14}$ Au/cm². The sample is amorphous with some phantoms of grain boundaries. **C**- Same area as in A *in situ* irradiated up to $2x10^{14}$ Au/cm². The sample is completely amorphous as shown by the homogenous contrast on the BF image and the presence of diffuse rings in the selected area electron diffraction (SAED) pattern (inset). **D**- Same area irradiated up to $5x10^{16}$ He/cm². Note the

presence of nuclei (arrows) that formed in the sample, and the corresponding diffraction spots (circle) reflecting recrystallization in the SAED pattern.

Figure 3. Bright-Field Transmission Electron Microscope images (BF-TEM) of a sequence of *in situ* irradiation in $LaPO_4$ monazite polycrystal - second experiment: intermediate irradiation dose ($5x10^{13}$ Au/cm²). **A-** Part of the TEM foil before irradiation with SAED pattern (inset). Note that some amorphous material is present in the sample due to the FIB preparation (diffuse ring in SAED). **B-** Same area as in A after one irradiation and annealing cycle (see Table in sup data) followed by this second cycle, which start with *in situ* irradiation up to $5x10^{13}$ Au/cm². The sample is still crystalline as demonstrated by the SAED pattern (inset) but contains more radiation damage as shown by the presence of diffuse rings in the SAED and the disappearance of Bragg diffraction lines in the BF image. **C** to **E-** Annealing cycle starting with irradiation of helium from $1x10^{14}$ He/cm² (C), $1x10^{15}$ He/cm² (D) to $5x10^{15}$ He/cm² (E). Note the progression of recrystallization with the disappearance of amorphous rings and appearance of Bragg diffraction lines, with well-defined bend contours at the end (E). After the last He-irradiation the sample is perfectly crystalline and the orientation has changed and is close to a zone axis (compare the SAED patterns). The presence of mottled diffraction contrasts attest for He irradiation. **F-** The entire foil after irradiation; the bottom-left part correspond to the previous observed areas. Note the upper right part masked to Au-irradiation (arrow), which testifies to original crystallinity of the sample.

Figure 4. BF-TEM of a sequence of *in situ* dual-beam (Au+He) irradiation in $LaPO_4$ monazite polycrystal. **A-** The entire foil before irradiation. **B-** Zoom in the left-bottom side area before irradiation. Note the Bragg diffraction lines (bend contours) witness of the crystallinity of the sample and depending on the orientation of the sample, and grain boundaries (sharp lines in the image). **C-** Simultaneous irradiation step with $1x10^{14}$ Au/cm² and $1.67x10^{16}$ He/cm². The sample is still crystalline (confirmed by SAED pattern), but with different bend contours resulting from slight orientation modification. **D-** Simultaneous irradiation step with $2x10^{14}$ Au/cm² and $3.40x10^{16}$ He/cm². The sample is still crystalline (confirmed by SAED pattern), with different bend contours. Note the presence of mottled diffraction contrasts in the upper part of the foil, which corresponds to few atomic displacements. **E-** The entire foil after dual-irradiation ($2x10^{14}$ Au/cm² and $3.40x10^{16}$ He/cm²). **F-** Zoom in the bottom-right area of the foil showing a large zone completely masked to He irradiation. A large part of this area is completely amorphous: homogeneous contrast in BF and diffuse rings in the SAED pattern performed inside the circle (inset in E).

This is a preprint, the final version is subject to change, of the American Mineralogist (MSA)
Cite as Authors (Year) Title. American Mineralogist, in press.
DOI: https://doi.org/10.2138/am-2018-6447

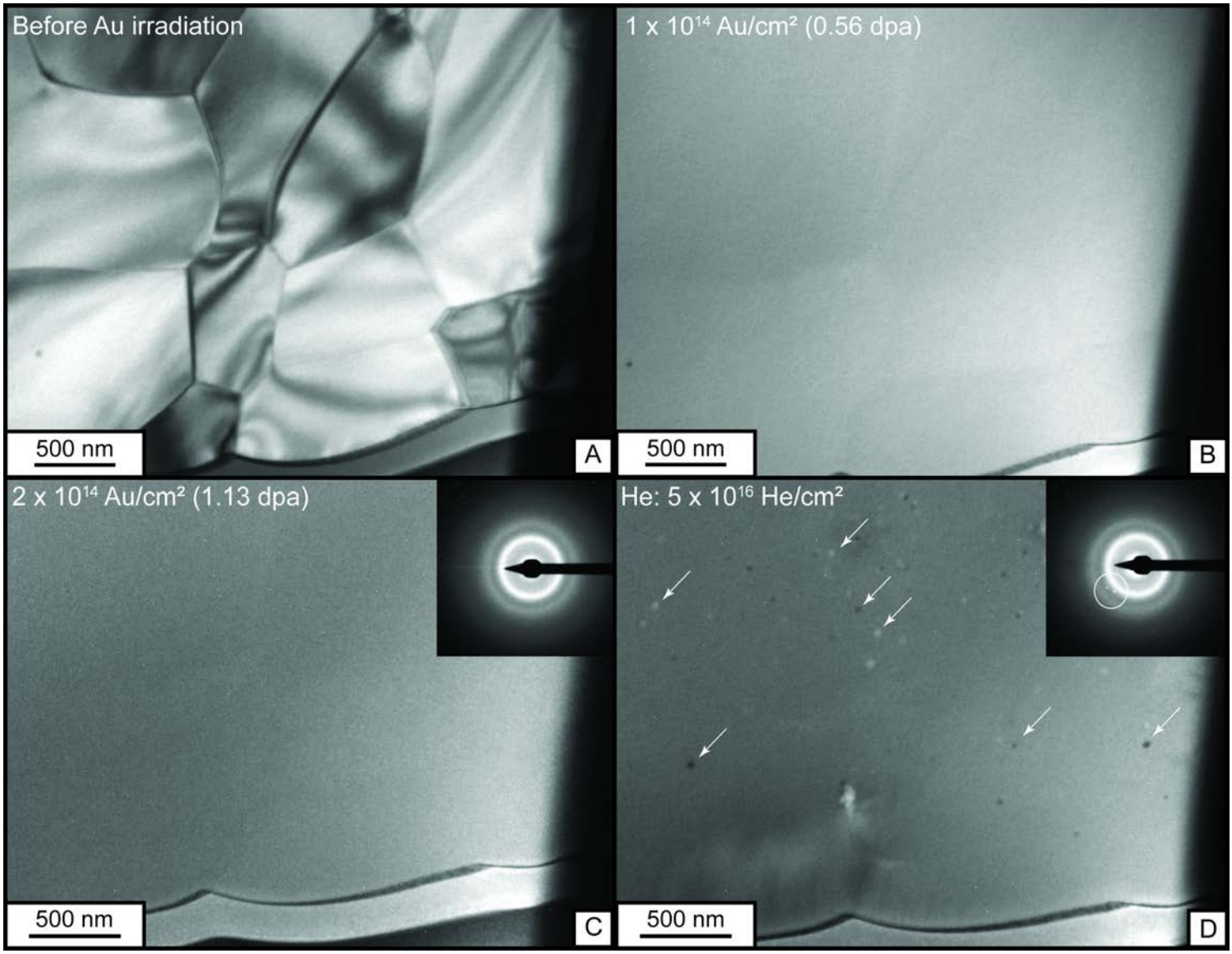

This is a preprint, the final version is subject to change, of the American Mineralogist (MSA)
Cite as Authors (Year) Title. American Mineralogist, in press.
DOI: https://doi.org/10.2138/am-2018-6447

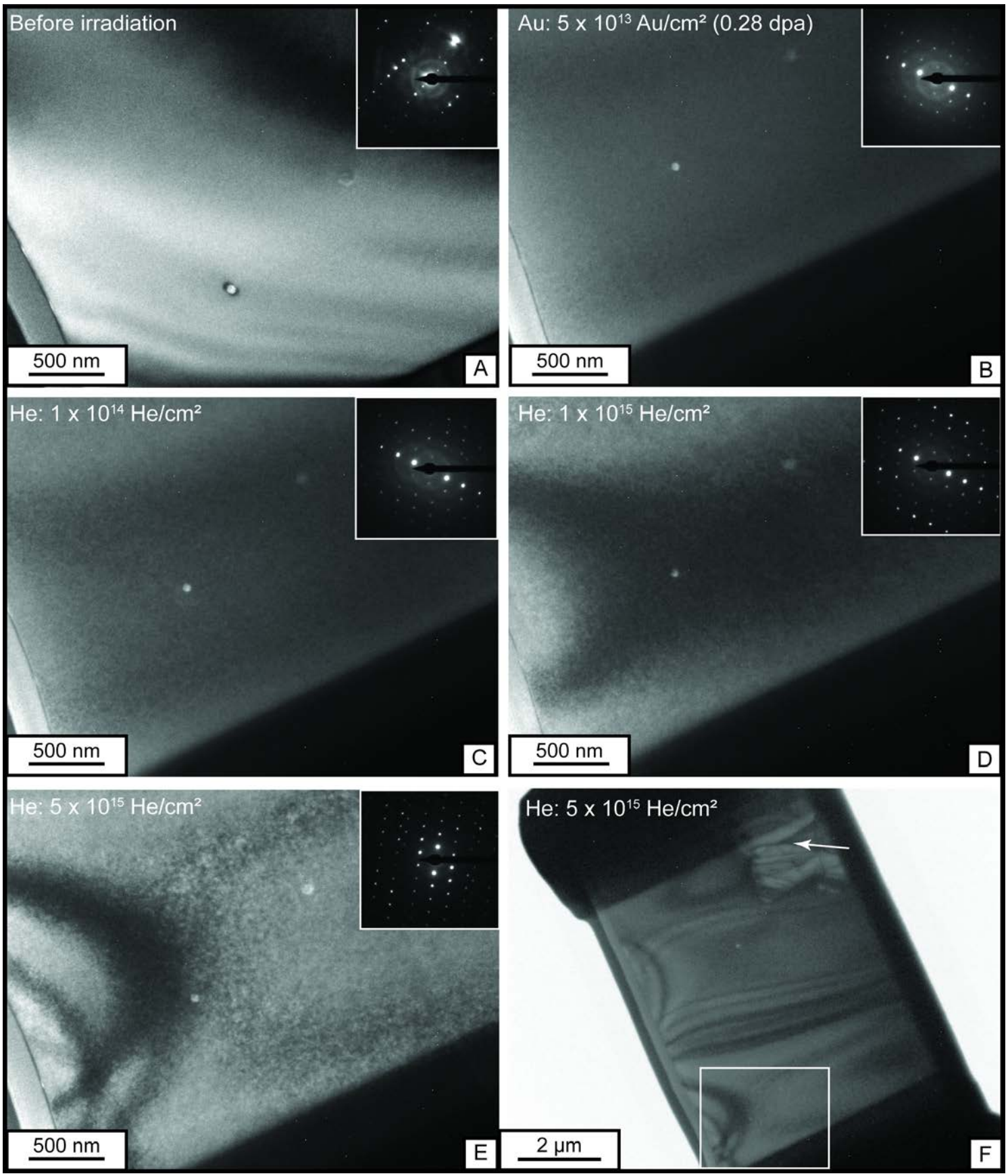

This is a preprint, the final version is subject to change, of the American Mineralogist (MSA)
Cite as Authors (Year) Title. American Mineralogist, in press.
DOI: https://doi.org/10.2138/am-2018-6447